Development 133, 2063-2073 (2006) doi:10.1242/dev.02374

Distinct cardiac malformations caused by absence of connexin 43 in the neural crest and in the non-crest neural tube

Shasha Liu[1], Fangyu Liu[1], Amanda E. Schneider[1], Tara St. Amand[1], Jonathan A. Epstein[2] and David E. Gutstein[1,3,*]

Connexin 43 (Cx43) is expressed in the embryonic heart, cardiac neural crest (CNC) and neural tube, and germline knockout (KO) of Cx43 results in aberrant cardiac outflow tract (OFT) formation and abnormal coronary deployment. Prior studies suggest a vital role for CNC expression of Cx43 in heart development. Surprisingly, we found that conditional knockout (CKO) of Cx43 in the dorsal neural tube and CNC mediated by Wnt1-Cre failed to recapitulate the Cx43-null OFT phenotype, although coronary vasculature was abnormal in this mutant line. A broader CKO mediated by P3pro (Pax3)-Cre, involving both ventral and dorsal aspects of the thoracic neural tube and CNC, resulted in infundibular bulging and coronary anomalies similar to those seen in germline Cx43-null hearts. P3pro-Cre-mediated loss of Cx43 in the neural tube was characterized by a late phase of cellular delamination from the dorsal and lateral neural tube, a markedly increased abundance of neuroepithelium-derived cells outside of the neural tube and an excess of such cells infiltrating the heart and infundibulum. Thus, expression of Cx43 in the CNC is crucial for normal coronary deployment, but Cx43 is not required in the CNC for normal OFT morphogenesis. Rather, this study suggests a novel function for Cx43 in which Cx43 acts through non-crest neuroepithelial cells to suppress cellular delamination from the neural tube and thereby preserve normal OFT development.

KEY WORDS: Connexin 43 (Gja1), Cardiac neural crest, Neural tube, Outflow tract, Heart defect, Mouse

INTRODUCTION

Connexins are membrane-spanning proteins that make up gap junctions – intercellular channels that allow ions, second messengers and other small molecules to pass between neighboring coupled cells (Goodenough et al., 1996). Gap junctions may play an important role in development by mediating the cell-to-cell transmission of signaling molecules involved in normal embryonic patterning (Lo and Wessels, 1998). Connexin 43 (Cx43; Gja1 – Mouse Genome Informatics) is the predominant cardiac connexin subtype in the latter stages of embryogenesis and postnatally (Gros and Jongsma, 1996; Severs et al., 1996). Cx43 has been implicated in human developmental disorders (Paznekas et al., 2003), although its role in congenital cardiac disease is controversial (Britz-Cunningham et al., 1995; Casey and Ballabio, 1995; Debrus et al., 1997; Splitt et al., 1995). Germline knockout (KO) of Cx43 in the mouse results in abnormal cardiac morphogenesis, including right ventricular outflow tract (OFT) abnormalities and perinatal death (Reaume et al., 1995).

We have previously observed that loss of Cx43 specifically in cardiomyocytes during embryogenesis is not associated with gross cardiac morphological defects at birth (Gutstein et al., 2001b). Although cardiomyocyte-restricted loss of Cx43 does not influence heart morphogenesis, affected mice had slowed interventricular electrical impulse conduction and were prone to spontaneous and inducible lethal ventricular arrhythmias (Danik et al., 2004; Gutstein et al., 2001b). Others have predicted that Cx43 expression may be required specifically in the cardiac neural crest (CNC) cells for normal heart morphogenesis (Ewart et al., 1997; Huang et al., 1998; Sullivan et al., 1998). The CNC is of vital importance in the development of the ventricular OFT and the great vessels. CNC cells migrate from the caudal pharyngeal arches into the common OFT of the developing heart tube, where they contribute to aorticopulmonary septation and other nearby structures (Hutson and Kirby, 2003). The importance of the CNC in cardiac morphogenesis is underscored by avian NC ablation, which produces profound morphological abnormalities of the aortic arch and ventricular OFT, as well as myocardial dysfunction (Kirby et al., 1983; Waldo et al., 1999).

Studies employing transgenic rescue and dominant-negative approaches have suggested that Cx43 expression in the NC may indeed influence cardiac morphogenesis (Ewart et al., 1997; Sullivan et al., 1998). However, patterns of activity of both the CMV-IE and EF-1α promoters used in these studies are not restricted to the NC cell lineage (Kim et al., 1990; Koedood et al., 1995; Kothary et al., 1991; Song et al., 1998). Furthermore, the Cx43-null mutant phenotype, characterized by infundibular bulging without septation defects, differs from other murine genetic models that affect CNC function. Genetic models including those with mutations in or knockouts of Pax3, neurotrophin 3/TrkC, TGFβ receptor type II, BMP4, BMP receptor IA, endothelin 1 and combinations of retinoic acid receptors (Choudhary et al., 2006; Donovan et al., 1996; Epstein et al., 2000; Kurihara et al., 1995; Liu et al., 2004; Mendelsohn et al., 1994; Stottmann et al., 2004; Youn et al., 2003) commonly cause OFT septation defects similar to those resulting from chick NC ablation. Thus, during development, Cx43 may be required in tissues that contribute to heart formation other than or in addition to the CNC (Li et al., 2002; Walker et al., 2005).

[1]Leon H. Charney Division of Cardiology, Department of Medicine, New York University School of Medicine, New York, NY 10016, USA. [2]Cardiovascular Institute, University of Pennsylvania, Philadelphia, PA 19104, USA. [3]Department of Cell Biology, New York University School of Medicine, New York, NY 10016, USA.

*Author for correspondence (e-mail: david.gutstein@nyumc.org)

Accepted 20 March 2006

To test the hypothesis that Cx43 expression in the CNC is crucial to normal heart development, we used parallel conditional knockout (CKO) strategies mediated by Wnt1-Cre and P3pro-Cre (driven by a proximal region of the Pax3 promoter) to generate lines of mice with CNC-restricted CKO of Cx43 (Epstein et al., 2000; Jiang et al., 2000; Li et al., 2000). Surprisingly, Wnt1-Cre-mediated CKO of Cx43 (Cx43-WCKO), which was limited to the dorsal neural tube (NT) and migrating NC cells, resulted in normal OFT development despite the presence of coronary anomalies. By contrast, P3pro-Cre-mediated CKO of Cx43 (Cx43-PCKO), which involved a broader dorsoventral domain of the thoracic NT, resulted in infundibular abnormalities similar to the germline Cx43 mutant, as well as aberrant coronary development. A late phase of delamination of Cx43-deficient P3pro-Cre-labeled cells was evident and an increased abundance of labeled cells were detected outside the NT in the Cx43-PCKO embryos. At E15.5, when OFT abnormalities were first noted in the Cx43-PCKO embryos, abundant labeled cells were detected in the heart, including the infundibulum. These data suggest that, in addition to effects on coronary deployment via expression in the CNC, Cx43 also acts through the non-crest neuroepithelium to suppress delamination of NT cells, which in the absence of Cx43 migrate aberrantly to the OFT and disrupt heart development.

MATERIALS AND METHODS

Wnt1- and P3pro-Cre-mediated CKO of Cx43

To investigate the role of Cx43 expression in the CNC during cardiac morphogenesis, we used the Cre-loxP system to generate Wnt1- and P3pro-Cre-mediated Cx43 CKO mice (Fig. 1A). For the generation of Cx43-WCKO mice, the Wnt1-Cre transgenic line was obtained as a generous gift from Dr H. Sucov (University of Southern California; with the permission of Dr A. McMahon, Harvard University) and crossed with Cx43 floxed mice (Gutstein et al., 2001b). Cx43-PCKO mice were generated by interbreeding the Cx43 floxed mice with P3pro-Cre transgenic mice, which use the proximal 1.6 kb of the Pax3 promoter to drive Cre recombinase expression (Epstein et al., 2000; Li et al., 2000). Cx43-WCKO and -PCKO lines were in similar mixed genetic backgrounds consisting of a mixture of 129/Sv, C57BL/6J and FVB strains. Mating strategies for Cx43-WCKO and -PCKO mice are shown in Fig. 1B,C, respectively. Cx43-WCKO and -PCKO lines were compared with control mice in the same strain background that carried two wild-type Cx43 alleles or had one or two floxed Cx43 alleles in the absence of Cre. The Cx43 floxed line generated in our laboratory has previously been shown to produce equivalent amounts of Cx43 in the heart when compared with wild-type littermates (Gutstein et al., 2001a). In addition, Cx43-PCKO mice were compared with littermates that were homozygous null ('floxed-out') for the Cx43 gene.

Genotypes were determined by Southern blotting and/or PCR of yolk sac or tail DNA using established techniques (Fig. 1D,E). All studies were performed in accordance with the regulations of the Institutional Animal Care and Use Committees of the New York University School of Medicine and the Veterans Administration New York Harbor Healthcare Medical Center (New York, NY).

Immunostaining for Cx43, Pax3 and Cre recombinase expression in CKO mice

For Cx43 immunostaining, embryos were fixed in 4% paraformaldehyde, equilibrated in sucrose and embedded in Tissue Tek OCT compound (Sakura Finetek USA, Torrance, CA) on dry ice. For the detection of Pax3 and Cre recombinase, embryos were fixed in 4% paraformaldehyde, dehydrated in graded alcohols and embedded in paraffin. Sections were blocked and incubated with primary antibodies, followed by fluorescence-conjugated secondary antibodies as described previously (Gutstein et al., 2003). Primary antibodies included a polyclonal anti-Cx43 antibody (Gutstein et al., 2003), a monoclonal anti-Pax3 antibody (Developmental Studies Hybridoma Bank, University of Iowa, Iowa City, IA) and a polyclonal anti-Cre recombinase antibody (Novagen, La Jolla, CA). Sections were mounted with Vectashield mounting medium (Vector Laboratories, Burlingame, CA). Samples were

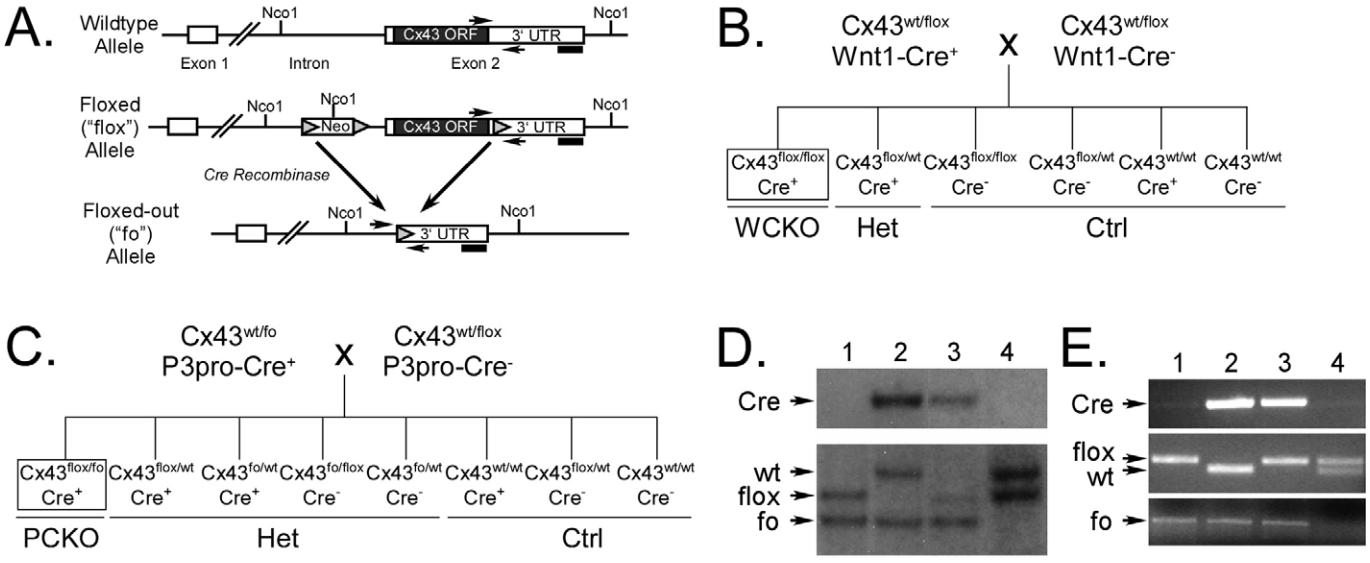

Fig. 1. Strategy for tissue-restricted conditional knockout (CKO) of Cx43. (**A**) Schematic representation of wild-type, floxed and floxed-out alleles, demonstrating the locations of *Nco*I sites, the probe used for Southern blotting (solid bar) and primer locations for PCR (small arrows). ORF, open reading frame; UTR, untranslated region. (**B**,**C**) Mating strategies for the generation of Wnt1- (B) and P3pro-Cre- (C) mediated CKO mice. Ctrl, control; flox, floxed; fo, floxed-out (Cx43-null). (**D**) Southern blotting of genomic DNA samples from tails of offspring from P3proCre^{+}:Cx43$^{fo/wt}$ × P3proCre^{-}:Cx43$^{flox/wt}$ matings. *Nco*I-digested genomic DNA yields a 6.5 kb wild-type band, a 5.4 kb floxed band and a 4.3 kb floxed-out band. Samples shown are from P3proCre^{-}:Cx43$^{flox/fo}$ (lane 1), P3proCre^{+}:Cx43$^{fo/wt}$ (lane 2), P3proCre^{+}:Cx43$^{flox/fo}$ (Cx43-PCKO; lane 3) and P3proCre^{-}:Cx43$^{flox/wt}$ pups (lane 4). (**E**) PCR samples showing similar genotypes to those in corresponding lanes in D. One primer pair is located entirely within exon 2 and generates a 220 bp PCR band from wild-type DNA and a 180 bp band from the floxed allele. A second primer pair generates a 550 bp product from the floxed-out allele and no product from either wild-type or floxed alleles.

visualized with an Axiovert 200M microscope (Carl Zeiss, Gottingen, Germany) equipped with appropriate filter blocks, which were chosen to avoid overlapping emission spectra.

Morphologic evaluation of CKO hearts

Whole explanted neonatal hearts were imaged to compare gross external appearance using a Leica MZ12.5 stereomicroscope equipped with a DEI-750D video camera (Leica, Wetzlar, Germany) with computer interface. Hearts were then washed in PBS and fixed in 4% paraformaldehyde. After ethanol dehydration and embedding in paraffin blocks, samples were sectioned at 5 μm. Selected sections were stained with Hematoxylin and Eosin using a Zeiss HMS Series Programmable Slide Stainer.

Detecting Cre transgene expression patterns in CKO mice

The EYFP-fluorescence Cre reporter strain (Srinivas et al., 2001) (kindly provided by Dr F. Costantini, Columbia University) was crossed into both the Cx43-PCKO and -WCKO lines. CKO embryos expressing the EYFP reporter construct were sectioned and imaged by fluorescence microscopy at E11.5 and E15.5.

In situ hybridization

Radioactive in situ hybridization for the detection of plexinA2 was performed according to the procedure available at http://www.uphs.upenn.edu/mcrc/histology/histologyhome.html, with probes that have been characterized elsewhere (Brown et al., 2001).

Statistics

Pup weights and cell density measurements (expressed as mean±s.d.) were compared with two-tailed *t*-tests using Microsoft Excel software. *P* values<0.05 were considered significant.

RESULTS

NC-specific loss of Cx43 expression in the Cx43-WCKO line

To investigate the tissue-restricted dependence of Cx43 expression for normal heart development, we have generated a mouse with conditional loss of Cx43 mediated by Wnt1-Cre (Cx43-WCKO mice) (Fig. 1A,B). Wnt1-Cre expression is restricted to the dorsal NT, which contributes to the NC (Jiang et al., 2000). Therefore, we predicted that cells derived from the NC lineage in Cx43-WCKO embryos would be deficient in Cx43. At E9.5, control embryos expressed abundant levels of Cx43 in the NC-derived cells of the pharyngeal arches (Fig. 2B,C). The distribution of Cx43 in the pharyngeal arches was largely punctate, consistent with patterns of Cx43 expression observed in cultured NC cells (Boot et al., 2006; Xu et al., 2001). As expected, pharyngeal arches of the Cx43-WCKO embryos at E9.5, in contrast to those of controls, were nearly devoid of Cx43 expression (Fig. 2E,F). Despite deficient Cx43 expression in the pharyngeal arches of Cx43-WCKO embryos, Cx43 immunosignal was preserved in the cardiac ventricles at E10.5 (Fig. 2G,H). Thus, Cx43 was efficiently knocked out in the NC lineage of the Cx43-WCKO mice.

Wnt1-Cre-mediated loss of Cx43 is associated with coronary anomalies

Coronary artery malformations have been described in both heterozygous and homozygous germline Cx43-null mice (Li et al., 2002; Walker et al., 2005). We investigated whether targeted loss of Cx43 using the Cx43-WCKO strategy might influence coronary patterning. In all eight control hearts examined at birth, a typical pattern of coronary deployment was observed. This pattern consisted of right and left coronary arteries originating from right and left coronary sinuses, respectively. Each coronary subsequently bifurcated into myocardial (including anterior descending and circumflex arteries on the left) and septal branches (Fig. 3A-D). By contrast, coronary abnormalities were observed in three out of five Cx43-WCKO hearts. These included separate ostia for right septal and myocardial coronary tributaries (Fig. 3E,F, respectively), an accessory coronary artery originating from the non-coronary sinus (Fig. 3G), and tunneling of the left coronary artery through the wall of the aorta (Fig. 3H), all of which have been described previously in germline Cx43-null mice (Li et al., 2002). These data suggest that expression of Cx43 in the NC is crucial for normal coronary development.

Wnt1-Cre-mediated loss of Cx43 does not result in infundibular defects

Based on data suggesting that Cx43 expression in the CNC lineage may be crucial for normal OFT development (Ewart et al., 1997; Huang et al., 1998; Sullivan et al., 1998), we predicted that Cx43-WCKO hearts would demonstrate infundibular abnormalities similar to the germline Cx43 mutant. Surprisingly, none of the 15 Cx43-

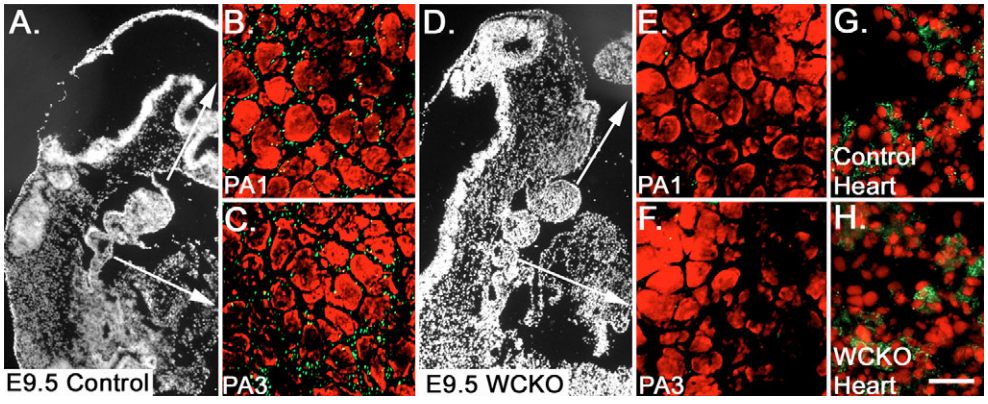

Fig. 2. Neural crest-specific knockout of Cx43 in Cx43-WCKO embryos. (**A**) Low-power, sagittal section of a wild-type E9.5 embryo demonstrating first, second and third pharyngeal arches. (**B**,**C**) Immunostaining for Cx43 (green stain) in high-power images of the first pharyngeal arch (PA1) (B) and the third pharyngeal arch (PA3) (C), in the E9.5 wild-type embryo. (**D**) Low-power image of an E9.5 Cx43-WCKO embryo. (**E**,**F**) High-power images of PA1 (E) and PA3 (F) in the E9.5 Cx43-WCKO embryo immunostained for Cx43. Cx43 signal is nearly absent in PA1 and PA3 in the Cx43-WCKO embryos in contrast to wild-type littermates. (**G**,**H**) Heart sections from E10.5 wild-type (G) and Cx43-WCKO (H) embryos immunostained for Cx43. Expression of Cx43 in the Cx43-WCKO heart is preserved at this stage. Propidium iodide nuclear staining is in red. Scale bar: 320 μm for A,D; 20 μm for B,C,E,F; 40 μm for G,H.

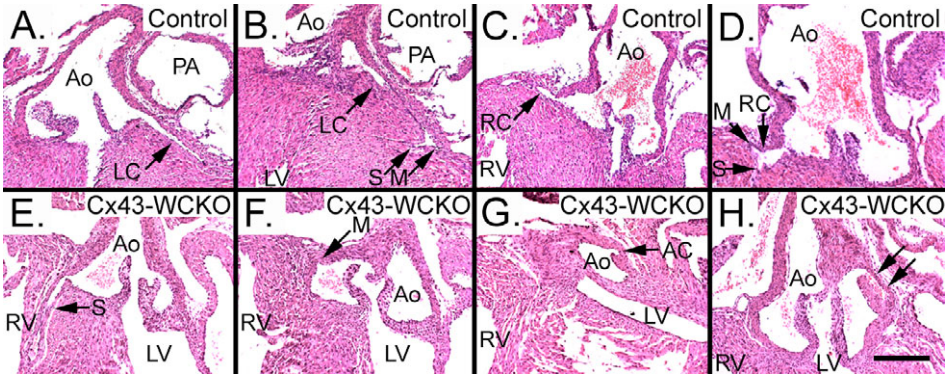

Fig. 3. Coronary anomalies in Cx43-WCKO neonatal hearts. (**A-D**) A typical pattern of coronary deployment in control mouse hearts is characterized by single left (A) and right (C) coronary ostia, each giving rise to arteries that bifurcate into left (B) and right (D) myocardial and septal branches. (**E-H**) Coronary abnormalities in Cx43-WCKOs included separate right septal (E) and myocardial branch ostia (F) in one heart, an accessory coronary (AC) originating from the non-coronary sinus in another heart (G), and tunneling of the left coronary artery through the wall of the aorta (arrows, H) in a third heart. Ao, aorta; PA, pulmonary artery; LC, left coronary artery; S, septal branch; M, myocardial branch; RC, right coronary artery; RV, right ventricle. Scale bar: 100 μm.

WCKO neonatal mice assayed had gross morphological or histological OFT abnormalities (Fig. 4). Thus, although expression of Cx43 in the dorsal NT and NC influences coronary deployment, Cx43 is not required in the Wnt1-Cre expression domain for normal OFT development. This suggests that expression of Cx43 in a cell population outside of the Wnt1-Cre expression domain is required to ensure normal OFT morphogenesis.

P3pro-Cre-mediated loss of Cx43

We next investigated whether a broader area of CKO than that seen in the Cx43-WCKO embryo might influence OFT development in addition to coronary deployment. We generated a mouse with conditional loss of Cx43 mediated by P3pro-Cre, the expression profile of which includes an expanded area of the NT compared with the Wnt1-Cre line (see Fig. 9). To produce P3pro-Cre-mediated Cx43 CKO (Cx43-PCKO) mice, P3proCre^{+} transgenic mice that were heterozygous null for Cx43 (P3proCre^{+}:Cx43$^{fo/wt}$) were crossed with mice harboring a floxed Cx43 gene locus on one allele (P3proCre^{-}:Cx43$^{flox/wt}$; Fig. 1C). Consistent with the known expression pattern of P3pro-Cre, abundance of Cx43 in the first pharyngeal arch was unchanged in Cx43-PCKO embryos (Fig. 5E) compared with littermate controls (Fig. 5B), but was drastically reduced around the third pharyngeal pouch of the Cx43-PCKO embryos (Fig. 5F). Cx43 expression in the E10.5 heart was unchanged in the targeted embryos (Fig. 5H) in comparison with controls (Fig. 5G).

At birth, Cx43-PCKOs were slightly but significantly smaller than their control littermates, although the mutant pups did not appear in distress. Mean neonatal Cx43-PCKO pup weights were decreased by 11.6% in comparison with heterozygous Cx43-null littermate controls (P<0.001). Genotypic analyses of pups from P3proCre^{+}:Cx43$^{fo/wt}$ × P3proCre^{-}:Cx43$^{flox/wt}$ matings (Fig. 1D,E) were expected to result in Cx43-PCKO mice (P3proCre^{+}:Cx43$^{fo/flox}$) with a frequency of 12.5%. Neonatal Cx43-PCKO pups were observed with a frequency of 9.0% (n=144 neonatal pups genotyped). However, only 4.6% of the pups genotyped at 2 weeks (n=359) carried the Cx43-PCKO genotype. Thus, Cx43-PCKO embryos demonstrate a restricted pattern of loss of Cx43 but die prematurely, suggesting a more severe phenotype than the Cx43-WCKOs.

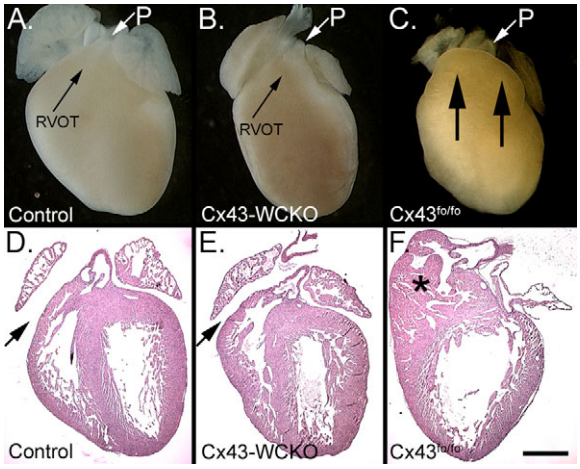

Fig. 4. Right ventricular outflow tract (RVOT) morphology of Cx43-WCKO hearts is grossly normal at birth. (**A-C**) Whole-mount images of control (A), Cx43-WCKO (B) and Cx43$^{fo/fo}$ (germline Cx43-null) (C) neonatal hearts. (**D-F**) Hematoxylin and Eosin-stained sections from control (D), Cx43-WCKO (E) and Cx43$^{fo/fo}$ (F) neonatal hearts. The Cx43-WCKO RVOT (arrow) appears similar to that of its littermate controls and lacks the infundibular bulging and exaggerated trabeculation (asterisk) seen in germline Cx43 KO hearts. P, pulmonary trunk; RVOT, right ventricular outflow tract. Scale bar: 1 mm.

Cx43-PCKO mice have gross right ventricular morphologic abnormalities

The morphological phenotype of the heart in neonatal Cx43-PCKO pups, consisting of a grossly mis-shapen RVOT, was remarkably similar to that of the germline Cx43 KO. Unlike in wild-type control hearts (Fig. 6E,F,L), large bulges were seen bilaterally flanking the OFT (indicated by arrows in Fig. 6A,C) in 20 out of 22 neonatal Cx43-PCKO hearts. Infundibular bulges characteristic of the Cx43-null hearts were not seen in any of the 27 wild-type control littermates and were observed in only one of 23 heterozygous Cx43 KO mice. Additionally, focal bulging segments were occasionally seen at the apices of neonatal Cx43-PCKO hearts (arrowhead in Fig. 6A), although similar apical outpouchings were seen in a minority of control littermates. Detailed examples of the infundibular bulges

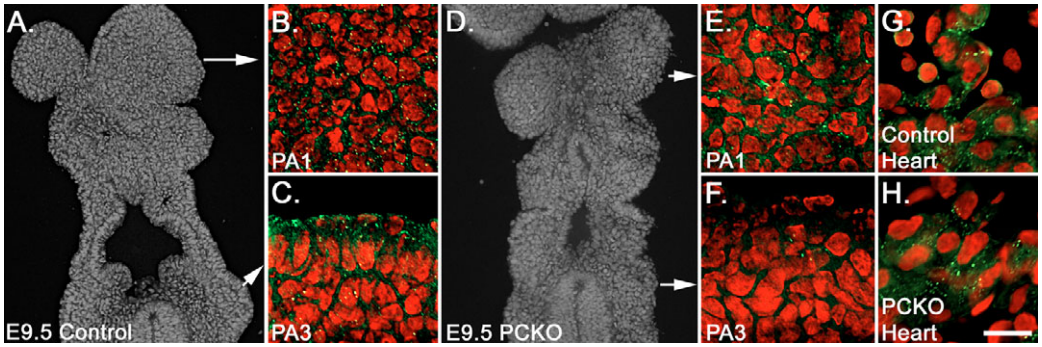

Fig. 5. Loss of Cx43 expression in Cx43-PCKO embryos involves the cardiac neural crest distribution. (**A**) Low-power image of a wild-type E9.5 embryo in cross-section demonstrating first, second and third pharyngeal arches. (**B**,**C**) Corresponding high-power images of the first pharyngeal arch (PA1) (B) and the third pharyngeal arch (PA3) (C) in the E9.5 wild-type embryo immunostained for Cx43 (green stain). (**D**) Low-power image of an E9.5 Cx43-PCKO embryo. (**E**,**F**) Corresponding high-power images of PA1 (E) and PA3 (F) in the E9.5 Cx43-PCKO embryo immunostained for Cx43. Cx43 signal is similar in PA1, but reduced in PA3 at E9.5 in the Cx43-PCKO embryos compared with wild-type littermates. (**G**,**H**) Heart sections from E10.5 wild-type (G) and Cx43-PCKO (H) embryos immunostained for Cx43. Expression of Cx43 in the Cx43-PCKO heart is preserved at this stage. Propidium iodide nuclear staining is in red. Scale bar: 200 μm for A,D; 20 μm for B,C,E-H.

were highlighted by the broken lines in Fig. 6B,D, where the contours of the ventricular walls just under the pulmonary trunk were seen to protrude prominently to either side. By contrast, the normal RVOT region tapered to form a triangular shape as it coursed into the pulmonic valve and pulmonary trunk. This pattern was seen in hearts from pups that were either wild type (Fig. 6E) or heterozygous null at the Cx43 locus (Fig. 6G). Higher magnification images demonstrated that the infundibular bulges seen in the Cx43-PCKO hearts were not present in either wild-type (Fig. 6F) or heterozygous Cx43-null hearts (Fig. 6H). However, infundibular bulges seen in the Cx43-PCKO hearts were comparable with those of the germline Cx43 KO hearts (Fig. 6I,J). Oblique views of Cx43-PCKO (Fig. 6K) and wild-type hearts (Fig. 6L) underscored the grossly altered contour of the mutant OFT when compared with that of the wild type. Thus, in addition to premature death, Cx43-PCKOs also share gross morphological features of their cardiac phenotype with germline Cx43 KOs.

Infundibular pouches underlie bulges and are first seen at E15.5 in the Cx43-PCKO mutant hearts

To fully characterize the abnormal RVOT development in the Cx43-PCKO mutant hearts, we evaluated sections at E13.5, E15.5, E17.5 and at birth (Fig. 7). At E13.5, the RVOT had an appearance unchanged in Cx43-PCKO and $Cx43^{fo/fo}$ germline KO hearts compared with control littermates (not shown). At E15.5, the RVOT in the Cx43-PCKO mouse first appeared abnormal. The base of the RV appeared more heavily trabeculated in Cx43-PCKO and $Cx43^{fo/fo}$ germline KO hearts (Fig. 7B,C) compared with controls (Fig. 7A). Furthermore, the infundibular myocardium of the Cx43-PCKO and $Cx43^{fo/fo}$ hearts had begun to bulge above the plane of the pulmonic valve (arrows in Fig. 7B,C), rather than taper gently into the pulmonic trunk, as was the case in control hearts (Fig. 7A).

Cell counts in the infundibulum at E15.5 revealed a trend towards increased cell density in the Cx43-PCKO compared with controls. Cell density in the infundibular regions of Cx43-PCKO hearts was

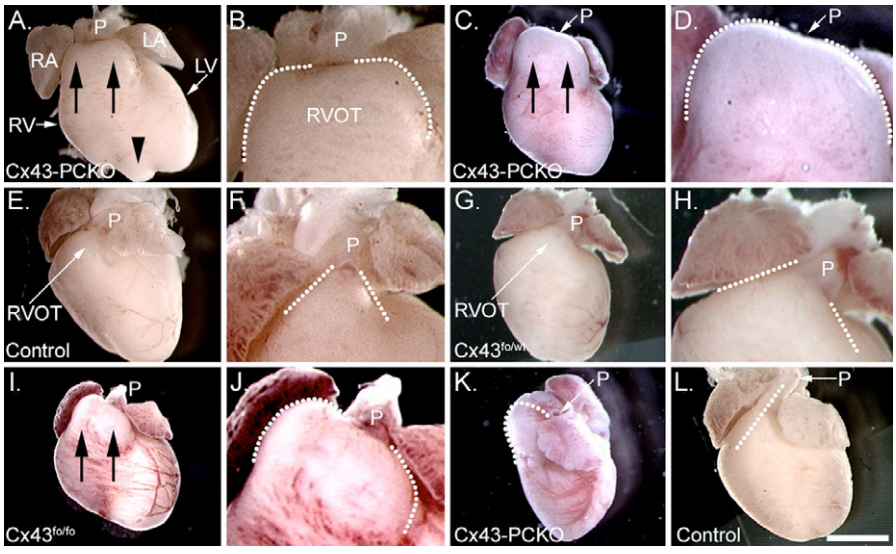

Fig. 6. Right ventricular morphology in Cx43-PCKO hearts is grossly abnormal. (**A**) Grossly visible bulges flanking the OFT are seen in Cx43-PCKO hearts (black arrows) and occasionally focal bulging segments at the right ventricular apex (arrowhead). (**B**) Detailed view of the RVOT in a Cx43-PCKO heart demonstrates grossly bulging infundibular contour. (**C**) Although most Cx43-PCKO hearts have infundibular bulges (arrows), many (including this heart) lack the bulging apical segment seen in A. (**D**) The RVOT region of the heart in C is markedly distorted. (**E**,**F**) Control and (**G**,**H**) $Cx43^{fo/wt}$ (heterozygous Cx43-null) hearts have grossly normal right ventricular and OFT morphology. Infundibular contours (outlined) form a triangular shape in the control and $Cx43^{fo/wt}$ hearts as they course towards the pulmonary trunk. (**I**,**J**) Infundibular bulges (arrows) in the Cx43-PCKO OFT are similar to those of the $Cx43^{fo/fo}$ (germline Cx43-null) heart. (**K**) Oblique view of the Cx43-PCKO RVOT demonstrates infundibular bulging above the level of the pulmonic valve. (**L**) By contrast, the contour of the wild-type RVOT tapers as it approaches the pulmonary trunk. P, pulmonary trunk; LA, left atrium; LV, left ventricle; RA, right atrium; RV, right ventricle; RVOT, right ventricular outflow tract. Scale bar: 1.2 mm for A,E,G,I,L; 750 μm for C,K; 400 μm for B,D,F,H,J.

4.5±1.6 cells/10 μm^2 (n=4), compared with a density of 3.5±0.7 cells/10 μm^2 (n=5) in controls. Although this difference was not statistically significant, in conjunction with upregulation of genes specific for vascular smooth muscle cells, endothelial cells and fibroblasts in Cx43 KO infundibular tissue (Walker et al., 2005), these data suggest an altered cellular composition of the mutant RVOTs. Infundibular bulging may result from such a change in cellular composition, which makes the RVOT unable to withstand increasing myocardial wall stress as development progresses.

At E17.5 and at birth, the infundibular abnormalities in the Cx43-PCKO more closely reflected the germline Cx43 KO appearance than at earlier stages. Cx43-PCKO and Cx43$^{fo/fo}$ OFTs were grossly deformed, with the ventricular wall adjacent to the pulmonic valve bulging prominently above the valve plane (arrows in Fig. 7E,F,K,L). In comparison with controls (Fig. 7D,J), the Cx43-PCKO and Cx43$^{fo/fo}$ OFTs appeared dilated and more densely trabeculated, with regions of the infundibular wall demonstrating considerable thinning. Although the LVOT of the Cx43-PCKO and Cx43$^{fo/fo}$ hearts (Fig. 7H,I, respectively) appeared similar to those of control hearts (Fig. 7G), the RV free wall was slightly thinner in the Cx43-PCKO and Cx43$^{fo/fo}$ hearts (asterisks in Fig. 7H,I) than in controls. Thus, the bulging infundibular phenotype, which is seen in both Cx43-PCKO and Cx43$^{fo/fo}$ embryos by E15.5, is more apparent in the Cx43$^{fo/fo}$ embryos at that initial stage, but appears similar in both mutant lines by E17.5.

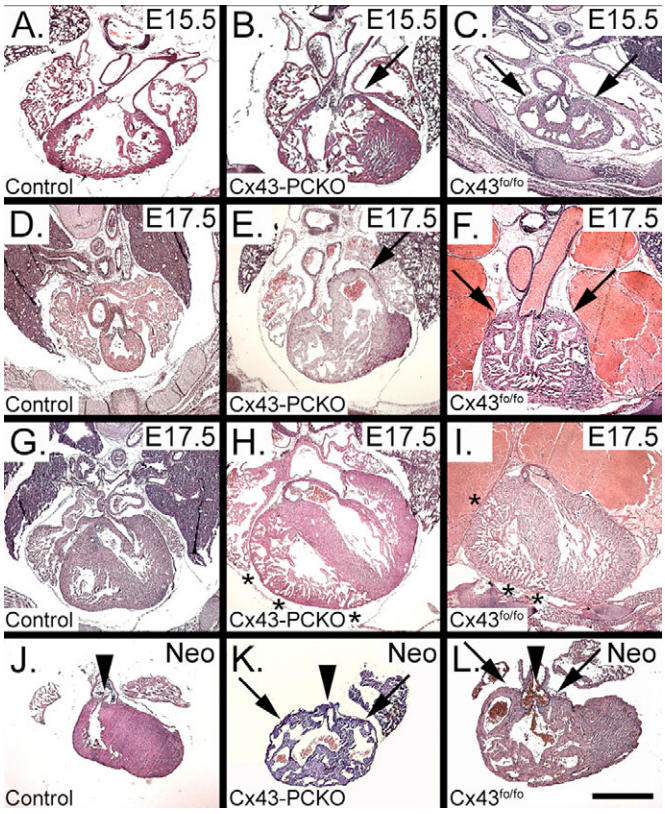

Fig. 7. Infundibular abnormalities are first seen at E15.5 in Cx43-PCKO hearts. (**A-C**) Hematoxylin and Eosin stained sections from E15.5 control (A), Cx43-PCKO (B) and Cx43$^{fo/fo}$ (C) hearts. Infundibular bulging is first apparent in the Cx43-PCKO and germline KO hearts at this stage (arrows in B and C). (**D-F**) Sections from control (D), Cx43-PCKO (E) and Cx43$^{fo/fo}$ (F) E17.5 hearts. The RVOT of the Cx43-PCKO heart is markedly deformed, as is that of the Cx43$^{fo/fo}$ heart (arrows in E and F, respectively). (**G-I**) Sections from control (G), Cx43-PCKO (H) and Cx43$^{fo/fo}$ (I) E17.5 hearts at the level of the LVOT. The Cx43-PCKO LVOT, like that of the Cx43$^{fo/fo}$ heart, appears similar to controls, although the RV-free walls of both the Cx43-PCKO and Cx43$^{fo/fo}$ hearts are thinned in comparison with controls (asterisks in H and I, respectively). (**J-L**) Sections through the RVOT of neonatal control (J), Cx43-PCKO (K) and Cx43$^{fo/fo}$ (L) hearts. The Cx43-PCKO RVOT is grossly dilated, heavily trabeculated (arrows) and bulges above the level of the pulmonic valve (arrowhead), unlike the control RVOT but similar to that of Cx43$^{fo/fo}$ hearts. Neo, neonatal. Scale bar: 450 μm for A-C,N; 700 μm for D-M,O.

Coronary anomalies are seen in Cx43-PCKO mice

As coronary anomalies are a prominent characteristic of the Cx43-null phenotype, we examined the coronary vasculature in the Cx43-PCKO hearts. In addition to OFT abnormalities, a wide variety of coronary abnormalities was evident in three out of five neonatal Cx43-PCKO hearts (Fig. 8A-H). In addition, tunneling of the right coronary artery through the wall of the aorta, another anomaly observed in germline Cx43 mutant mice (Li et al., 2002), was incidentally noted in an E17.5 Cx43-PCKO (Fig. 8I-K).

Numerous coronary abnormalities have previously been described in heterozygous Cx43-null mice (Li et al., 2002). As the Cx43-PCKO mice are in a heterozygous Cx43-null background, we examined Cx43$^{fo/wt}$ hearts for evidence of coronary anomalies. In fact, two out of five Cx43$^{fo/wt}$ hearts demonstrated myocardial and septal coronary arteries originating from the same ostium on the aorta, rather than branching from a main coronary artery (Fig. 8L), a finding previously noted in heterozygous Cx43-null mice (Li et al., 2002). In summary, Cx43-PCKOs share a number of phenotypic features with germline Cx43 KO mice, including coronary anomalies, infundibular bulging and perinatal death.

Late phase of cellular delamination from the neural tube in Cx43-PCKOs

Given the dramatic morphological differences between the Cx43-WCKO and -PCKO lines, we investigated how the expression patterns of Cre recombinase in the CKO embryos might impact on their phenotypes. Cells expressing Cre were fluorescence labeled by crossing an EYFP Cre reporter strain (Srinivas et al., 2001) into the Cx43-PCKO and -WCKO lines. Cells derived from P3pro-Cre expressing precursors were located throughout the thoracic NT (Fig. 9A; EYFP is represented by green fluorescence, propidium iodide to highlight cell nuclei is red and their overlap results in yellow signal). By contrast, cells derived from Wnt1-Cre expressing precursors were primarily limited to the dorsal NT (Fig. 9J). Surprisingly, P3pro-Cre-expressing cells were delaminating from the dorsal and lateral aspects of the NT in the Cx43-PCKO embryos at E11.5 (Fig. 9E,F), a phenomenon also observed in Cx43 germline KO (Cx43$^{fo/fo}$) embryos at this stage (Fig. 9G-I). Cellular delamination from the NT was not seen in control littermates (Fig. 9B,C,K,L) or in Cx43-WCKO embryos (Fig. 9N,O) at this stage. These data suggest that Cx43 is required in areas of the NT outside of the Wnt1-Cre expression domain in order to maintain normal neuroepithelial cell behavior.

Increased abundance of migrating neuroepithelial cells in the Cx43-PCKO embryo

Loss of Cx43 was associated with an increased abundance of EYFP-labeled cells outside the NT at E11.5 in the Cx43-PCKO embryos (Fig. 10C) compared with controls (Fig. 10A). In addition to an increased abundance of labeled cells, the normal distribution of labeled cells in the Cx43-PCKO embryos appeared disrupted. For

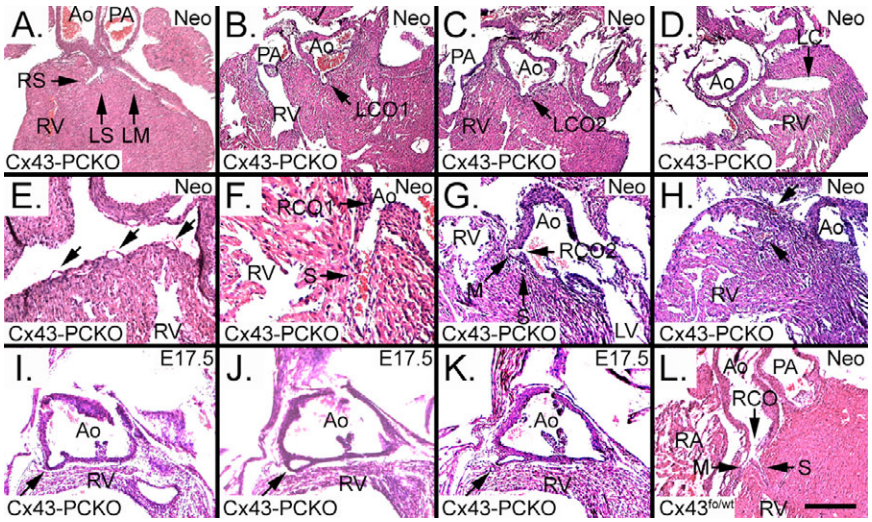

Fig. 8. Coronary patterning is altered in Cx43-PCKO hearts. (**A**) One neonatal Cx43-PCKO heart has a right septal branch (RS) that originates from the left coronary artery. (**B-E**) Two separate coronary ostia are seen in the left coronary sinus of one of the Cx43-PCKO neonatal hearts (B,C). One ostium (LCO1) gives rise to a septal artery (B); the other (LCO2) gives rise to a large, aneurysmal artery that traverses the bulging tissue of the infundibulum (C,D). This mutant heart also has a blistering appearance of the right ventricular lateral wall, possibly consistent with subepicardial coronary plexuses described in the germline Cx43-null heart (arrows, E) (Walker et al., 2005). (**F-H**) Another neonatal Cx43-PCKO heart has dual right coronary ostia. One ostium (RCO1) leads to a large septal artery (F). The second right coronary ostium (RCO2) gives rise to a septal branch and a myocardial tributary (G), which subsequently divides into branches that cross through the RV infundibulum (arrows, H). (**I-K**) Tunneling of the right coronary artery (arrows) through the wall of the aorta is shown in an E17.5 Cx43-PCKO heart. (**L**) Two out of five neonatal heterozygous Cx43-null ($Cx43^{fo/wt}$) hearts demonstrated coronary artery branching at the ostium. Ao, aorta; LC, left coronary artery; LCO, left coronary ostium; LM, left myocardial branch; LS, left septal branch; LV, left ventricle; M, myocardial branch; PA, pulmonary artery; RA, right atrium; RC, right coronary artery; RCO, right coronary ostium; RV, right ventricle; S, septal branch. Scale bar: 225 μm for A-D; 112.5 μm for E,G-L; 56 μm for F.

example, in control embryos at E11.5, the trachea at the level of the OFT was flanked by discrete collections of labeled cells that appeared to be streaming into the OFT (Fig. 10B), as previously described (Epstein et al., 2000). By contrast, labeled cells in the Cx43-PCKO embryo at this stage were greatly increased in abundance and have extensively infiltrated the paratracheal tissue in close proximity to the OFT (Fig. 10D). The disordered distribution of labeled cells observed in the Cx43-PCKO embryos was not seen in Cx43-WCKOs (see Fig. 10F; compare with $Wnt1\text{-}Cre^{+}$ controls in Fig. 10E).

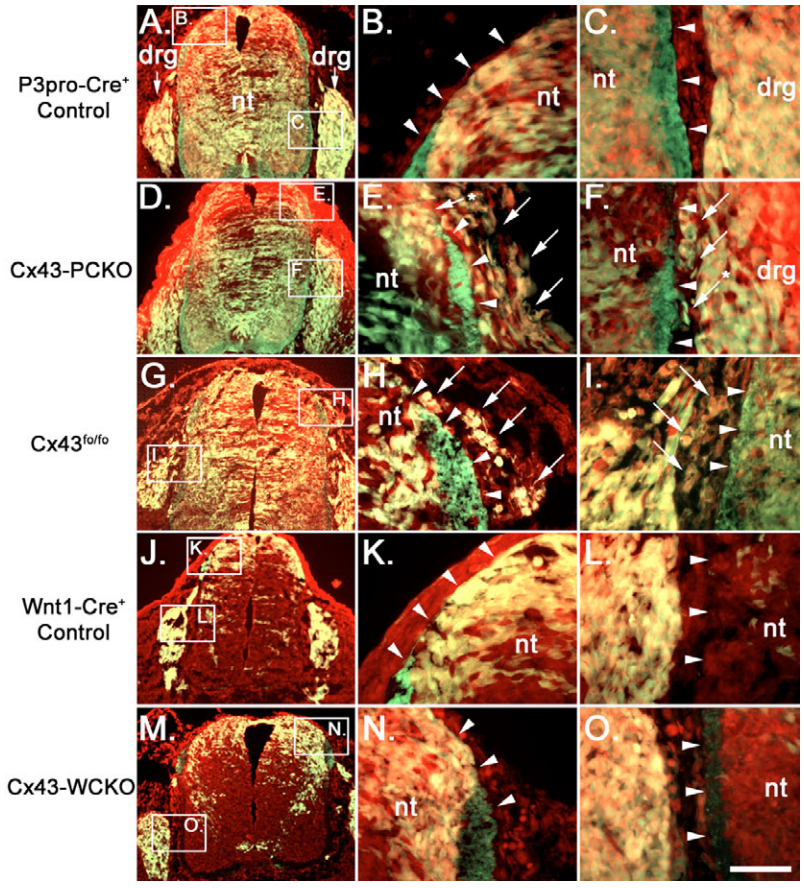

Fig. 9. Exuberant delamination of neuroepithelial cells in E11.5 Cx43-PCKO embryos. (**A-F**) P3pro-Cre-expressing control (A) and Cx43-PCKO E11.5 embryos (D), crossed into the EYFP Cre reporter line demonstrate extensive Cre activity throughout the neural tube (nt) and dorsal root ganglia (drg). High-power views of the dorsal (B) and lateral (C) aspects of the control neural tube shown in A demonstrate a sharp boundary at the neuroepithelial border (arrowheads). No cells crossing this boundary are seen. In contrast to controls, neural tube cells in the E11.5 Cx43-PCKO embryo are delaminating from the dorsal (E) and lateral (F) aspects of the neural tube (arrows; asterisked arrow indicates an actively delaminating cell). (**G-I**) As observed in the Cx43-PCKOs, delamination of cells from Cx43 germline KO ($Cx43^{fo/fo}$) neural tubes (G) is detected along the dorsal (H) and lateral (I) surfaces. (**J-O**) Wnt1-Cre activity is limited primarily to the dorsal regions of E11.5 EYFP-expressing control (J) and Cx43-WCKO (M) neural tubes. Labeled cells are not seen outside either dorsal or lateral aspects of the $Wnt1\text{-}Cre^{+}$ control (K,L) or Cx43-WCKO (N,O) neural tubes. EYFP fluorescence appears green, propidium iodide to highlight cell nuclei is red and their overlap results in yellow signal. Scale bar: 200 μm for A,D,G,J,M; 50 μm for all other panels.

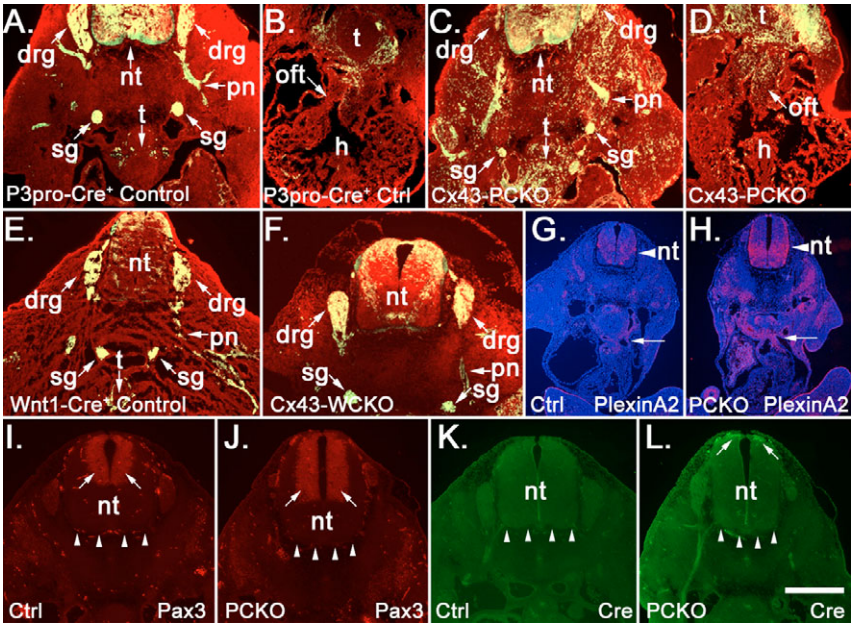

Fig. 10. Increased abundance of neuroepithelium-derived cells in the E11.5 Cx43-PCKO embryo. (**A**) Wild-type E11.5 expression pattern of P3pro-Cre^{+}:Cx43$^{+/+}$, EYFP-labeled cells (green signal) are limited to the neural tube, dorsal root ganglia (drg), peripheral nerves (pn), sympathetic ganglia (sg) and small circumscribed collections of labeled cells flanking the trachea (t) and esophagus. Sections in A-F are counterstained with propidium iodide to highlight the nuclei; overlap with EYFP appears as yellow signal. (**B**) Labeled cells flanking the trachea are shown migrating into the OFT of a control E11.5 embryo. (**C**) Section from an E11.5 Cx43-PCKO EYFP embryo at the level of the heart, showing an increased abundance of labeled cells outside of the neural tube in comparison with the control littermate. (**D**) Labeled cells are abundant in and around the tracheal region adjacent to the OFT in the Cx43-PCKO embryo at E11.5. (**E**,**F**) Labeled cells in sections from E11.5 Wnt1-Cre^{+} control (E) and Cx43-WCKO embryos (F) at the level of the heart share a similar distribution to that of P3pro-Cre^{+} controls, except in the neural tube where the Wnt1-Cre^{+} cells have a more limited distribution. (**G**) Radioactive in situ hybridization of E11.5 control embryos shows plexin A2 mRNA (pink) distributed in the neural tube (arrowhead) and in the OFT (arrow), as well as in paratracheal tissue adjacent to the OFT. (**H**) In contrast to the control embryos, Cx43-PCKO embryos express higher levels of plexin A2 (pink) in the neural tube (arrowhead), OFT (arrow) and paratracheal tissue, as well as elsewhere in the embryo. (**I**,**J**) Immunostaining for the presence of Pax3 (red) in control (I) and Cx43-PCKO (J) sections (indicated by arrows) at E11.5 reveals an unchanged expression pattern in the mutant embryos. (**K**) Cre recombinase expression (green) is absent in control embryos. (**L**) Cre expression is seen primarily at the dorsal aspect of the neural tube in Cx43-PCKO embryos at this stage (arrows). Arrowheads indicate the ventral boundary of the neural tube. Scale bar: 200 μm for A-F; 100 μm for G,H; 400 μm for I-L.

To help determine whether EYFP-labeled cells outside of the E11.5 Cx43-PCKO NT were neuroepithelial in origin, we evaluated the expression of plexin A2, a semaphorin receptor expressed in migratory and postmigratory NT-derived cells (Brown et al., 2001). In control embryos, plexin A2 expression was detected by in situ hybridization in the NT (arrowhead, Fig. 10G) and in the cells entering the cardiac OFT (arrow). In Cx43-PCKO embryos, expression of plexin A2 was more abundant, particularly in the NT (arrowhead, Fig. 10H) and in cells adjacent to the OFT (arrow). Increased expression of plexin A2 in the Cx43-PCKO embryos correlated well with the increased abundance of EYFP-labeled cells observed around the OFT at E11.5. Thus, neuroepithelial cells appear to be migrating through the Cx43-PCKO embryo at E11.5 in substantially greater numbers than in control embryos.

To investigate whether altered P3pro-Cre transgene activity in Cx43-PCKO embryos might contribute to the increase in EYFP-labeled cells outside of the NT, we immunostained E11.5 specimens for both Pax3 and Cre recombinase. As demonstrated in Fig. 10I, the native Pax3 expression domain in controls is limited to the dorsal and medial regions of the NT at E11.5. This expression pattern is unchanged in Cx43-PCKO littermates, and there is no discernible increase in Pax3 expression outside of the NT in Cx43-PCKOs (Fig. 10J). Cre recombinase expression is absent in control specimens, as expected (Fig. 10K). In E11.5 Cx43-PCKOs, Cre immunosignal is primarily limited to a small region of the Pax3 expression domain at the dorsal aspect of the NT (Fig. 10L) with scattered and less intense expression in cells in the medial and ventral NT. These data suggest that increased EYFP-labeled cells outside of the NT in Cx43-PCKO embryos do not derive from ectopic P3pro-Cre transgene activity, but rather result from the loss of Cx43 in the non-crest neuroepithelium.

Extensive infiltration of EYFP-labeled cells in E15.5 Cx43-PCKO hearts

EYFP-labeled cells in control embryos expressing the P3pro-Cre transgene at E15.5 were largely confined to the OFT region (Fig. 11A,B). EYFP-labeling mediated by Wnt1-Cre in control (Fig. 11E,F) and Cx43-WCKO E15.5 hearts (Fig. 11G,H), like that seen in the P3pro-Cre-expressing controls, demonstrated a limited presence of labeled cells in the septal region of the OFT, adjacent to the aortic valve. EYFP-positive cells were detected only rarely in the RV infundibulum of the P3pro-Cre-expressing controls, Wnt1-Cre-expressing controls and Cx43-WCKOs (arrows in Fig. 11A,B,E-H). By contrast, abundant labeled cells in the Cx43-PCKO embryos at E15.5 have infiltrated the infundibular myocardium and other areas of the heart (Fig. 11C,D). Thus, in contrast to controls and Cx43-WCKO embryos, Cx43-PCKO embryos had an increased abundance of labeled cells, some of which appeared to have delaminated aberrantly from the NT, migrated abnormally and ultimately incorporated into the heart. These data strongly argue for a novel function of Cx43 on NT regions outside of the Wnt1-Cre expression domain in regulating neuroepithelial cell behavior.

DISCUSSION

In the present study, we tested the hypothesis that Cx43 expression in the CNC is crucial to normal heart development. To our surprise, we found that although loss of Cx43 in the dorsal NT and CNC resulted in coronary anomalies, it did not recapitulate the bulging RVOT morphologic phenotype of the germline Cx43 KO. Rather, an expanded area of loss of Cx43 in the NT mediated by P3pro-Cre resulted in both coronary anomalies and the bulging RVOT phenotype. P3pro-Cre-mediated loss of Cx43 was associated with a late phase of delamination from the NT, abundant aberrantly

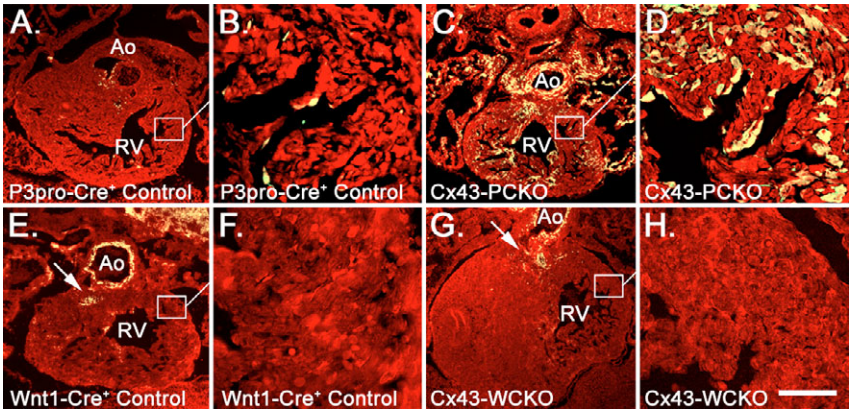

Fig. 11. Extensive infiltration of labeled cells into the E15.5 Cx43-PCKO heart. (**A**) Short axis section through the RV infundibulum in an E15.5 P3pro-Cre$^+$ control embryo showing labeled cells primarily limited to the area adjacent to the aortic valve. (**B**) Higher magnification of the infundibular myocardium in A (boxed) demonstrates only rare labeled cells. (**C**) RVOT of an E15.5 Cx43-PCKO embryo showing abundant labeled cells infiltrating the myocardium. (**D**) Higher magnification of the indicated region in C demonstrates numerous labeled cells in the myocardial wall and trabeculae. (**E-H**) Short axis sections through the RV infundibulum in a Wnt1-Cre$^+$ control (E,F) and a Cx43-WCKO heart (G,H) reveal a limited distribution of labeled cells (arrows) similar to that seen in the P3pro-Cre$^+$ control. F,H are higher magnifications of the boxed areas in E,G. Ao, aorta; RV, right ventricle. Scale bar: 400 μm for A,C,E,G; 50 μm for B,D,F,H.

migrating neuroepithelium-derived cells and eventual incorporation of those cells into the infundibulum of the heart. These data suggest that Cx43 acts through the non-crest neuroepithelium to regulate the ability of NT cells to undergo transformation into mesenchyme, migrate from the tube and ultimately influence morphogenesis of the heart.

Increased plexin A2 expression in the Cx43-PCKO embryo suggests that the increased abundance of EYFP-labeled cells outside of the NT derives from neuroepithelium. These late-delaminating cells differ from NC cells in that they emerge from the NT after NC cells have ceased to delaminate. Thus, in the normal state, Cx43 expression in the NT appears to be involved in suppressing the process by which these late-delaminating cells emerge from the tube. The effect of Cx43 on neuroepithelial behavior may be mediated through a direct effect on intracellular signaling or, indirectly, via intercellular coupling. A number of intermediaries, such as SoxE transcription factors, sonic hedgehog (Shh), BMPs acting through Wnt signaling and TGFβ, have been implicated in the control of crucial processes related to neuroepithelial patterning and differentiation (Cayuso et al., 2006; Chesnutt et al., 2004; Cheung et al., 2005; McKeown et al., 2005; Testaz et al., 2001). However, a direct role for connexin proteins in these signaling pathways in the NT has not been reported previously. Alternatively, Cx43 gap junctions may allow for the intercellular transfer of neuroepithelial regulatory signals. In the absence of gap junctions, such signals may be less able to diffuse through the NT as the embryo grows, leading to a late phase of delamination.

As an initial step to help distinguish the lineage responsible for the Cx43-null phenotype, we have previously used a targeted approach to delete Cx43 expression specifically in cardiomyocytes with two separate cardiac-specific Cre recombinase mouse lines, MLC-2v-Cre (Chen et al., 1998) and α-MHC-Cre (Agah et al., 1997). Both MLC-2v-Cre and α-MHC-Cre are expressed in the heart prior to E9 (Chen et al., 1998; de Lange et al., 2004). Despite an 85-95% reduction in cardiac Cx43 expression, cardiac-specific Cx43 CKO mice are grossly and histologically indistinguishable from their non-KO littermates and have normal ventricular function by echocardiography. Although the cardiac-specific Cx43 CKO mice are structurally normal, they demonstrate slowed intracardiac conduction and began to die suddenly and spontaneously, starting at 2-3 weeks of age from ventricular arrhythmias (Danik et al., 2004; Gutstein et al., 2001b). Thus, Cx43 expression in cardiomyocytes does not appear to be necessary for normal cardiac morphogenesis.

Other studies using dominant-negative (Sullivan et al., 1998) and transgenic overexpression approaches (Ewart et al., 1997; Huang et al., 1998) have suggested that Cx43 expression in the CNC is of crucial importance to OFT development. However, important differences exist between the phenotypes of the dominant-negative mutant and the germline Cx43 KO, which may result from nonspecific effects of a dominant-negative approach. Transgenic rescue of the germline Cx43-null mouse is incomplete and data from this approach are necessarily obfuscated by the unknown effects on cell function of overexpression of Cx43. In addition, patterns of activity of both the EF-1α and CMV-IE promoters used for the dominant-negative and overexpression studies, respectively, are not restricted to the NC cell lineage (Guo et al., 1996; Kim et al., 1990; Koedood et al., 1995; Kothary et al., 1991; Song et al., 1998). Wnt1-Cre, however, allowed for a much more precise evaluation of the role of the CNC in the Cx43-null phenotype (Jiang et al., 2000). Despite the near-complete loss of Cx43 expression in the NC-derived pharyngeal arches of the Cx43-WCKO embryos, heart morphology was normal, although coronary patterning was altered.

Previous work by others has established that Cx43 plays an important role in coronary artery development (Li et al., 2002; Walker et al., 2005). Our study suggests that the effect of Cx43 on coronary patterning is mediated through its expression in the NC. As NC cells invest the proximal regions of murine coronary arteries (Jiang et al., 2000), loss of Cx43 may influence ostial coronary development by directly regulating crest cell function. Alternatively, crest cells may exert an indirect effect on coronary artery patterning through epicardial cells via a gap junction-dependent mechanism (Gittenberger-de Groot et al., 2004; Walker et al., 2005). Either way, the effect of Cx43 on NC cell biology vis-à-vis coronary development may prove to be clinically relevant. Isolated anomalies of the coronary arteries have been associated with sudden death and exercise-related death, particularly in young athletes (Frescura et al., 1998; Maron et al., 1996; Taylor et al., 1992).

Recently, other investigators have described a population of migratory cells that emerge from the ventral NT and contribute widely to the formation of visceral organs, vascular structures and connective tissue (reviewed by Dickinson et al., 2004). These ventrally emigrating NT (VENT) cells, the existence of which is highly controversial (Boot et al., 2003; Yaneza et al., 2002), are thought to emerge from the ventral NT at sites of nerve exit. As labeled NT cells in the Cx43-PCKO embryos appear to be delaminating from the dorsal and lateral aspects of the NT, however, regulatory pathways involving Cx43 probably differ from those of the VENT cells.

In conclusion, by comparing tissue-restricted CKOs of Cx43 using Wnt1-Cre and P3pro-Cre, we have found that Cx43 expression in the non-crest NT plays a key role in OFT morphogenesis in the embryonic mouse. Our findings suggest that the Cx43 gap junction protein acts through the non-crest neuroepithelium to regulate transformation, delamination and/or migration in NT cells, and indirectly influences heart development as a result.

The authors thank Drs Margaret L. Kirby, Cecilia W. Lo, Glenn I. Fishman and Dina C. Myers for helpful discussions. This work was supported by NIH grants HL61475 (to J.A.E.) and HL081336, and by a Grant-in-Aid from the American Heart Association (to D.E.G.).

References

Agah, R., Frenkel, P. A., French, B. A., Michael, L. H., Overbeek, P. A. and Schneider, M. D. (1997). Gene recombination in postmitotic cells. Targeted expression of Cre recombinase provokes cardiac-restricted, site-specific rearrangement in adult ventricular muscle in vivo. *J. Clin. Invest.* **100**, 169-179.

Boot, M. J., Gittenberger-de Groot, A. C., van Iperen, L. and Poelmann, R. E. (2003). The myth of ventrally emigrating neural tube (VENT) cells and their contribution to the developing cardiovascular system. *Anat. Embryol.* **206**, 327-333.

Boot, M. J., Gittenberger-de Groot, A. C., Poelmann, R. E. and Gourdie, R. G. (2006). Connexin43 levels are increased in mouse neural crest cells exposed to homocysteine. *Birth Defects Res. Part A Clin. Mol Teratol.* **76**, 133-137.

Britz-Cunningham, S. H., Shah, M. M., Zuppan, C. W. and Fletcher, W. H. (1995). Mutations of the connexin43 gap-junction gene in patients with heart malformations and defects of laterality. *N. Engl. J. Med.* **332**, 1323-1329.

Brown, C. B., Feiner, L., Lu, M. M., Li, J., Ma, X., Webber, A. L., Jia, L., Raper, J. A. and Epstein, J. A. (2001). PlexinA2 and semaphorin signaling during cardiac neural crest development. *Development* **128**, 3071-3080.

Casey, B. and Ballabio, A. (1995). Connexin43 mutations in sporadic and familial defects of laterality. *N. Engl. J. Med.* **333**, 941-942.

Cayuso, J., Ulloa, F., Cox, B., Briscoe, J. and Marti, E. (2006). The Sonic hedgehog pathway independently controls the patterning, proliferation and survival of neuroepithelial cells by regulating Gli activity. *Development* **133**, 517-528.

Chen, J., Kubalak, S. W. and Chien, K. R. (1998). Ventricular muscle-restricted targeting of the RXRalpha gene reveals a non-cell-autonomous requirement in cardiac chamber morphogenesis. *Development* **125**, 1943-1949.

Chesnutt, C., Burrus, L. W., Brown, A. M. and Niswander, L. (2004). Coordinate regulation of neural tube patterning and proliferation by TGFbeta and WNT activity. *Dev. Biol.* **274**, 334-347.

Cheung, M., Chaboissier, M. C., Mynett, A., Hirst, E., Schedl, A. and Briscoe, J. (2005). The transcriptional control of trunk neural crest induction, survival, and delamination. *Dev. Cell* **8**, 179-192.

Choudhary, B., Ito, Y., Makita, T., Sasaki, T., Chai, Y. and Sucov, H. M. (2006). Cardiovascular malformations with normal smooth muscle differentiation in neural crest-specific type II TGFbeta receptor (Tgfbr2) mutant mice. *Dev. Biol.* **289**, 420-429.

Danik, S. B., Liu, F., Zhang, J., Suk, H. J., Morley, G. E., Fishman, G. I. and Gutstein, D. E. (2004). Modulation of cardiac gap junction expression and arrhythmic susceptibility. *Circ. Res.* **95**, 1035-1041.

de Lange, F. J., Moorman, A. F., Anderson, R. H., Manner, J., Soufan, A. T., de Gier-de Vries, C., Schneider, M. D., Webb, S., van den Hoff, M. J. and Christoffels, V. M. (2004). Lineage and morphogenetic analysis of the cardiac valves. *Circ. Res.* **95**, 645-654.

Debrus, S., Tuffery, S., Matsuoka, R., Galal, O., Sarda, P., Sauer, U., Bozio, A., Tanman, B., Toutain, A., Claustres, M. et al. (1997). Lack of evidence for connexin 43 gene mutations in human autosomal recessive lateralization defects. *J. Mol. Cell. Cardiol.* **29**, 1423-1431.

Dickinson, D. P., Machnicki, M., Ali, M. M., Zhang, Z. and Sohal, G. S. (2004). Ventrally emigrating neural tube (VENT) cells: a second neural tube-derived cell population. *J. Anat.* **205**, 79-98.

Donovan, M. J., Hahn, R., Tessarollo, L. and Hempstead, B. L. (1996). Identification of an essential nonneuronal function of neurotrophin 3 in mammalian cardiac development. *Nat. Genet.* **14**, 210-213.

Epstein, J. A., Li, J., Lang, D., Chen, F., Brown, C. B., Jin, F., Lu, M. M., Thomas, M., Liu, E., Wessels, A. et al. (2000). Migration of cardiac neural crest cells in Splotch embryos. *Development* **127**, 1869-1878.

Ewart, J. L., Cohen, M. F., Meyer, R. A., Huang, G. Y., Wessels, A., Gourdie, R. G., Chin, A. J., Park, S. M., Lazatin, B. O., Villabon, S. et al. (1997). Heart and neural tube defects in transgenic mice overexpressing the Cx43 gap junction gene. *Development* **124**, 1281-1292.

Frescura, C., Basso, C., Thiene, G., Corrado, D., Pennelli, T., Angelini, A. and Daliento, L. (1998). Anomalous origin of coronary arteries and risk of sudden death: a study based on an autopsy population of congenital heart disease. *Hum. Pathol.* **29**, 689-695.

Gittenberger-de Groot, A. C., Eralp, I., Lie-Venema, H., Bartelings, M. M. and Poelmann, R. E. (2004). Development of the coronary vasculature and its implications for coronary abnormalities in general and specifically in pulmonary atresia without ventricular septal defect. *Acta Paediatr. Suppl.* **93**, 13-19.

Goodenough, D. A., Goliger, J. A. and Paul, D. L. (1996). Connexins, connexons, and intercellular communication. *Annu. Rev. Biochem.* **65**, 475-502.

Gros, D. B. and Jongsma, H. J. (1996). Connexins in mammalian heart function. *BioEssays* **18**, 719-730.

Guo, Z. S., Wang, L. H., Eisensmith, R. C. and Woo, S. L. (1996). Evaluation of promoter strength for hepatic gene expression in vivo following adenovirus-mediated gene transfer. *Gene Ther.* **3**, 802-810.

Gutstein, D. E., Morley, G. E. and Fishman, G. I. (2001a). Conditional gene targeting of connexin43: exploring the consequences of gap junction remodeling in the heart. *Cell Commun. Adhes.* **8**, 345-348.

Gutstein, D. E., Morley, G. E., Tamaddon, H., Vaidya, D., Schneider, M. D., Chen, J., Chien, K. R., Stuhlmann, H. and Fishman, G. I. (2001b). Conduction slowing and sudden arrhythmic death in mice with cardiac-restricted inactivation of connexin43. *Circ. Res.* **88**, 333-339.

Gutstein, D. E., Liu, F. Y., Meyers, M. B., Choo, A. and Fishman, G. I. (2003). The organization of adherens junctions and desmosomes at the cardiac intercalated disc is independent of gap junctions. *J. Cell Sci.* **116**, 875-885.

Huang, G. Y., Wessels, A., Smith, B. R., Linask, K. K., Ewart, J. L. and Lo, C. W. (1998). Alteration in connexin 43 gap junction gene dosage impairs conotruncal heart development. *Dev. Biol.* **198**, 32-44.

Hutson, M. R. and Kirby, M. L. (2003). Neural crest and cardiovascular development: a 20-year perspective. *Birth Defects Res. C Embryo Today* **69**, 2-13.

Jiang, X., Rowitch, D. H., Soriano, P., McMahon, A. P. and Sucov, H. M. (2000). Fate of the mammalian cardiac neural crest. *Development* **127**, 1607-1616.

Kim, D. W., Uetsuki, T., Kaziro, Y., Yamaguchi, N. and Sugano, S. (1990). Use of the human elongation factor 1 alpha promoter as a versatile and efficient expression system. *Gene* **91**, 217-223.

Kirby, M. L., Gale, T. F. and Stewart, D. E. (1983). Neural crest cells contribute to normal aorticopulmonary septation. *Science* **220**, 1059-1061.

Koedood, M., Fichtel, A., Meier, P. and Mitchell, P. J. (1995). Human cytomegalovirus (HCMV) immediate-early enhancer/promoter specificity during embryogenesis defines target tissues of congenital HCMV infection. *J. Virol.* **69**, 2194-2207.

Kothary, R., Barton, S. C., Franz, T., Norris, M. L., Hettle, S. and Surani, M. A. (1991). Unusual cell specific expression of a major human cytomegalovirus immediate early gene promoter-lacZ hybrid gene in transgenic mouse embryos. *Mech. Dev.* **35**, 25-31.

Kurihara, Y., Kurihara, H., Oda, H., Maemura, K., Nagai, R., Ishikawa, T. and Yazaki, Y. (1995). Aortic arch malformations and ventricular septal defect in mice deficient in endothelin-1. *J. Clin. Invest.* **96**, 293-300.

Li, J., Chen, F. and Epstein, J. A. (2000). Neural crest expression of Cre recombinase directed by the proximal Pax3 promoter in transgenic mice. *Genesis* **26**, 162-164.

Li, W. E., Waldo, K., Linask, K. L., Chen, T., Wessels, A., Parmacek, M. S., Kirby, M. L. and Lo, C. W. (2002). An essential role for connexin43 gap junctions in mouse coronary artery development. *Development* **129**, 2031-2042.

Liu, W., Selever, J., Wang, D., Lu, M. F., Moses, K. A., Schwartz, R. J. and Martin, J. F. (2004). Bmp4 signaling is required for outflow-tract septation and branchial-arch artery remodeling. *Proc. Natl. Acad. Sci. USA* **101**, 4489-4494.

Lo, C. W. and Wessels, A. (1998). Cx43 gap junctions in cardiac development. *Trends Cardiovasc. Med.* **8**, 264-269.

Maron, B. J., Shirani, J., Poliac, L. C., Mathenge, R., Roberts, W. C. and Mueller, F. O. (1996). Sudden death in young competitive athletes. Clinical, demographic, and pathological profiles. *Jama* **276**, 199-204.

McKeown, S. J., Lee, V. M., Bronner-Fraser, M., Newgreen, D. F. and Farlie, P. G. (2005). Sox10 overexpression induces neural crest-like cells from all dorsoventral levels of the neural tube but inhibits differentiation. *Dev. Dyn.* **233**, 430-444.

Mendelsohn, C., Lohnes, D., Decimo, D., Lufkin, T., LeMeur, M., Chambon, P. and Mark, M. (1994). Function of the retinoic acid receptors (RARs) during

development (II). Multiple abnormalities at various stages of organogenesis in RAR double mutants. *Development* **120**, 2749-2771.
Paznekas, W. A., Boyadjiev, S. A., Shapiro, R. E., Daniels, O., Wollnik, B., Keegan, C. E., Innis, J. W., Dinulos, M. B., Christian, C., Hannibal, M. C. et al. (2003). Connexin 43 (GJA1) mutations cause the pleiotropic phenotype of oculodentodigital dysplasia. *Am. J. Hum. Genet.* **72**, 408-418.
Reaume, A. G., de Sousa, P. A., Kulkarni, S., Langille, B. L., Zhu, D., Davies, T. C., Juneja, S. C., Kidder, G. M. and Rossant, J. (1995). Cardiac malformation in neonatal mice lacking connexin43. *Science* **267**, 1831-1834.
Severs, N. J., Dupont, E., Kaprielian, R. R., Yeh, H. I. and Rothery, S. (1996). Gap junctions and connexins in the cardiovascular system. In *Annual of Cardiac Surgery 1996* (9th edn) (ed. M. H. Yacoub, A. Carpentier, J. Pepper and J. N. Fabiani), pp. 31-44. London: Current Science.
Song, S., Morgan, M., Ellis, T., Poirier, A., Chesnut, K., Wang, J., Brantly, M., Muzyczka, N., Byrne, B. J., Atkinson, M. et al. (1998). Sustained secretion of human alpha-1-antitrypsin from murine muscle transduced with adeno-associated virus vectors. *Proc. Natl. Acad. Sci. USA* **95**, 14384-14388.
Splitt, M. P., Burn, J. and Goodship, J. (1995). Connexin43 mutations in sporadic and familial defects of laterality. *N. Engl. J. Med.* **333**, 941-942.
Srinivas, S., Watanabe, T., Lin, C. S., William, C. M., Tanabe, Y., Jessell, T. M. and Costantini, F. (2001). Cre reporter strains produced by targeted insertion of EYFP and ECFP into the ROSA26 locus. *BMC Dev. Biol.* **1**, 4.
Stottmann, R. W., Choi, M., Mishina, Y., Meyers, E. N. and Klingensmith, J. (2004). BMP receptor IA is required in mammalian neural crest cells for development of the cardiac outflow tract and ventricular myocardium. *Development* **131**, 2205-2218.
Sullivan, R., Huang, G. Y., Meyer, R. A., Wessels, A., Linask, K. K. and Lo, C. W. (1998). Heart malformations in transgenic mice exhibiting dominant negative inhibition of gap junctional communication in neural crest cells. *Dev. Biol.* **204**, 224-234.
Taylor, A. J., Rogan, K. M. and Virmani, R. (1992). Sudden cardiac death associated with isolated congenital coronary artery anomalies. *J. Am. Coll. Cardiol.* **20**, 640-647.
Testaz, S., Jarov, A., Williams, K. P., Ling, L. E., Koteliansky, V. E., Fournier-Thibault, C. and Duband, J. L. (2001). Sonic hedgehog restricts adhesion and migration of neural crest cells independently of the Patched- Smoothened-Gli signaling pathway. *Proc. Natl. Acad. Sci. USA* **98**, 12521-12526.
Waldo, K., Zdanowicz, M., Burch, J., Kumiski, D. H., Stadt, H. A., Godt, R. E., Creazzo, T. L. and Kirby, M. L. (1999). A novel role for cardiac neural crest in heart development. *J. Clin. Invest.* **103**, 1499-1507.
Walker, D. L., Vacha, S. J., Kirby, M. L. and Lo, C. W. (2005). Connexin43 deficiency causes dysregulation of coronary vasculogenesis. *Dev. Biol.* **284**, 479-498.
Xu, X., Li, W. E., Huang, G. Y., Meyer, R., Chen, T., Luo, Y., Thomas, M. P., Radice, G. L. and Lo, C. W. (2001). Modulation of mouse neural crest cell motility by N-cadherin and connexin 43 gap junctions. *J. Cell Biol.* **154**, 217-230.
Yaneza, M., Gilthorpe, J. D., Lumsden, A. and Tucker, A. S. (2002). No evidence for ventrally migrating neural tube cells from the mid- and hindbrain. *Dev. Dyn.* **223**, 163-167.
Youn, Y. H., Feng, J., Tessarollo, L., Ito, K. and Sieber-Blum, M. (2003). Neural crest stem cell and cardiac endothelium defects in the TrkC null mouse. *Mol. Cell Neurosci.* **24**, 160-170.